Optimizing SIFT algorithm parameters for better matching UAV and satellite images

Optimizing SIFT algorithm parameters for better matching UAV and satellite images

K A Elorabi[1,a], A Zekry[2] and WA Mohamed[1]

[1]Benha Faculty of Engineering, Benha University, Benha, Egypt
[2]Ain Shams Faculty of Engineering, Ain Shams University, Cairo, Egypt
[a]kamalorabi@yahoo.com

Abstract. Image registration has been increasingly employed in various applications such as target identification, 3D mapping, and motion tracking. The main idea of Image registration is aligning two or more images of the same scene captured from different viewpoints, at different times. Scale-invariant feature transform, SIFT, is considered one of the most robust algorithms used in image registration for extracting and matching features under different conditions. Using SIFT algorithm default parameters in Matching UAV and satellite Images provides unreliable results due to the nature of aerial images because the dynamic range is quite low. The number of extracted features depends on the image content and the selected parameters. In this paper we tuned SIFT parameters to get the best performance with aerial images, to increase the number of features (SM) and the correct match rate (CMR) which increases the efficiency of the process of registration. The algorithm is validated by matching a large number of aerial images taken by mini-UAV with satellite images for the same region.

Keywords: image registration; matching images; SIFT.

1. Introduction

The Unmanned Aerial Vehicle (UAV) can fly remotely without a pilot on board; the presence of the pilot is compensated using avionics on the UAV and electronic equipment in the GCS (Ground Control Station) to control the UAV directly from the ground. Thinking about UAVs started in the '50s for use in military applications. During the cold war, many countries started to think about producing a drone capable of carrying out missions without a pilot on board. With the technological development, these days UAVs are used in many civilian and military fields, due to the advantages of UAVs such as low cost, usage in dangerous areas, long endurance of up to 30 hours, capturing images at low altitudes with a low speed which gives us very high precision images and reduces the exposure risk of the aircraft pilot,… etc. The main goal of the UAVs is to capture images and videos for the surveillance area to identify important targets. To achieve this goal image registration is the most important technique used to match UAV images with images from other sources such as satellite images. The main image

registration idea is aligning two or more images of the same scene captured from different viewpoints, at different times, and with different sensors. Despite Image, Registration has been widely discussed in the last 10 years, and many methods have been proposed, it is still an open problem. the contribution of this paper is tuning SIFT parameters to match the characteristics of the aerial images to increase the number of features (SM) and the correct match rate (CMR) which increases the efficiency of the process of registration. The proposed parameters achieve the best results when compared with the default parameters proposed by Lowe in the process of registering aerial images with satellite images from Google Earth.
We organized this paper as follows. In Section 2, we reviewed the related work. Then we described the methodology in Section 3. In Section 4, we presented the experimental results and discussions. Finally, section 5 contains the conclusion and future work.

2. Related work

The correlations between different images depend on features extracting distinctive features from each image. These features are known as points of interest. The area around each feature is known as the interest region which is invariant to changes in rotation, illumination, and scaling. The numbers of extracted features depend on the nature of the images and the used parameters. So interest points become a popular tool for detecting objects, creating 3D models, and creating panoramas [1]. The creation of panoramas is one of the most popular applications for feature extraction because under normal conditions we need the images to be in order and have the same viewpoint and scale. However, depending on the local feature extraction panoramas may be created automatically with no need for the previous conditions.
Another application for image registration is image mosaicking, where we can make a new image by combining two or more images such that the new image is less distorted than the original images. The creation of 3d maps is also one of the most important applications for image registration, where 3d mapping has been developed by the Swedish defense and security company Saab. Navigation by using 2D maps cannot meet the requirement for robot navigation because of the lack of navigation data [2].
Nowadays, there are large numbers of interest region detectors. The selection of which one of them will be used depends on the needed application. Remondino has tested six regions and interest point detectors. The result of this test proved that the SIFT algorithm is one of the best region detectors in extracting points of interest [3] and [4]. Lowe used the least square matching algorithm (LSM) to improve SIFT accuracy by using the Euclidean distance. A key point from the first image is chosen, and another two Key points are chosen from the second image. The selection of these two points depends on whether they have the shortest and next-shortest Euclidean distances between these two features. If the value between the two distances is less than a predefined threshold the pair of features is considered matched. The matching is considered stable if the result between the second distance and the first one is more than the threshold value. Speed Up Robust Features (SURF) is robust for limited changes in the image scale and rotation, but not when the images present many rotations like aerial images taken from UAVs due to the movement of the drone [5] and [6]. There are some optimized algorithms from SIFT, for example, Principal Components Analysis PCA-SIFT [7] and [8]. The descriptor in PCA-SIFT is more compact than SIFT, which speeds up the matching process. However, it is still sensitive to variations in scale and blur. The evaluation of SIFT algorithm in the previous research was focused on the variance of illumination and the geometric of the images, but they ignored the texture distribution or the dynamic range. The aerial images are considered bad textured because the dynamic range is quite low. Lowe proposed some parameters that these parameters should be tuned to match the characteristics of the aerial images. The number of features depends on the image content and the selected parameters. This number of features is very important in the process of registration. SIFT has 17 parameters. Tuning all the parameters would be a very complex job, so authors usually select the most effective parameters for tuning [9] and [10]. SIFT takes more time in the process of registration than other algorithms like

SURF, but authors agree that SIFT is a very robust algorithm against image variation and can be used in many applications [11] and [12].

3. METHODOLOGY

3.1. The SIFT Algorithm

SIFT algorithm is used to find the correspondence between images [13]. This algorithm compares and matches the detected features in the input image with the features in the target image to make a robust match between them. These features are not affected by distortion, scaling, blurring, rotation, or illumination. SIFT algorithm flowchart is shown in figure 1.

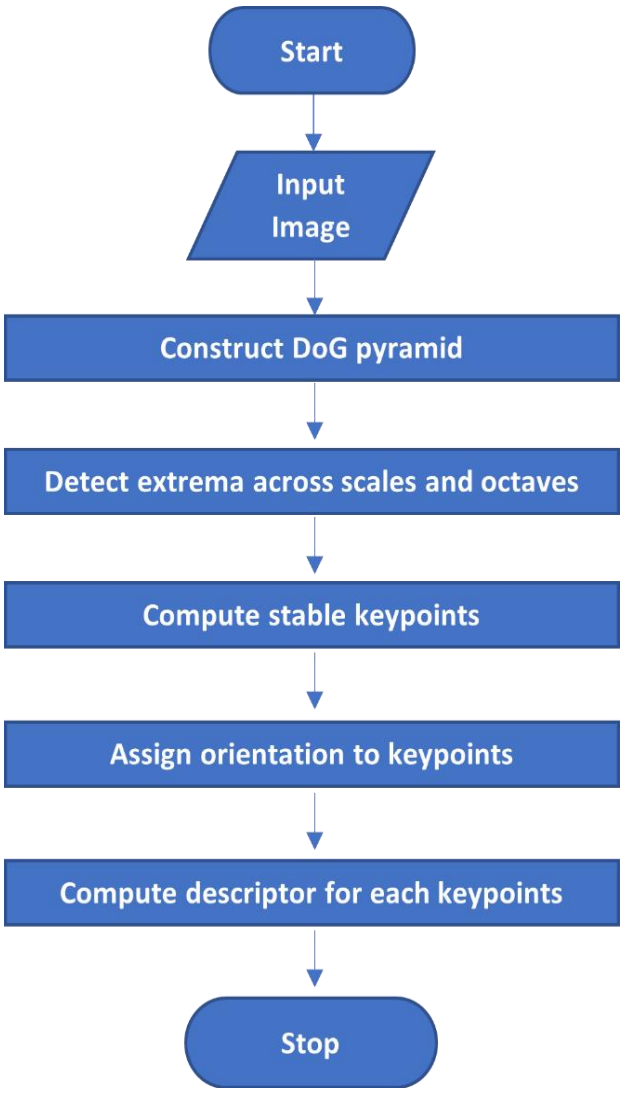

Figure 1. Flowchart of the SIFT algorithm.

3.2. SIFT algorithm Main stages

- **Scale-space extrema detection.** In this stage, we Search over multiple scales and image locations to identify potential interest points that are invariant to scale and orientation. the creation of the Gaussian scale-space pyramid is the first step by using the convolution of Gaussian functions to produce sequential blurred images (octave) as shown in equation (1) and equation (2). The parameter of n-Scales represents the number of scales inside the octave. The parameter sigma (σ) is responsible for the initial Gaussian blur for the first level of each octave [13]. Thus, the Gaussian scale-space can be represented as several images each of them representing a different zoom scale as shown in figure 2.

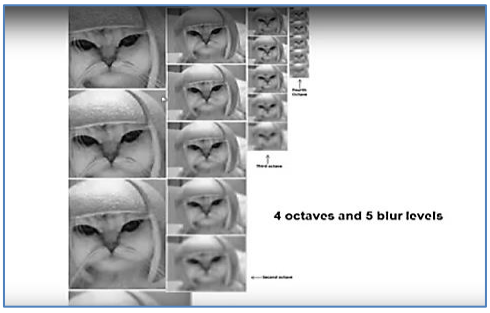

Figure 2. Constructing a Scale Space.

The scale-space of an image is defined as a function, L(x, y, σ), that is produced from the convolution of a variable-scale Gaussian, G(x, y, σ), with an input image, I(x, y):

$$L(x, y, \sigma) = G(x, y, \sigma) * I(x, y) \quad (1)$$

$$G(x, y, \sigma) = \frac{1}{2\pi\sigma^2} e^{-(x^2+y^2)/2\sigma^2} \quad (2)$$

Where (L) is the blurred image, (G) is the Gaussian bluer operator, (I) is an image, (X, Y) is the location coordinates, and (σ) is the amount of bluer (greater the value greater the bluer).

- **Difference of Gaussian (DOG).** We use scale space from the previous step to calculate the difference between two consecutive scales to find interesting key points in the images as shown in figure 3.

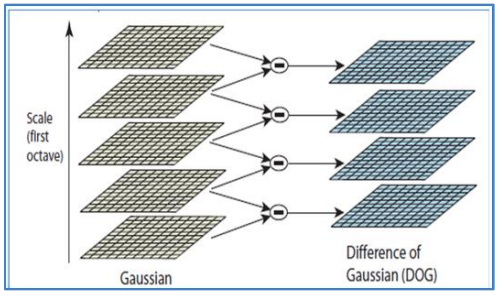

Figure 3. Difference of Gaussian (DOG).

D(x, y, σ), compute the difference of two nearby scales separated by a constant multiplicative factor k as shown in equation (3).

$$D(x, y, \sigma) = (G(x, y, k\sigma) - G(x, y, \sigma)) * I(x, y)$$
$$= L(x, y, k\sigma) - L(x, y, \sigma) \quad (3)$$

- **Feature localization**. In this stage, the initial features are selected by comparing each point to its 26 neighbors and looking for extrema as shown in figure 4. The number of features is reduced by eliminating the features along edges or in low-contrast regions [13].

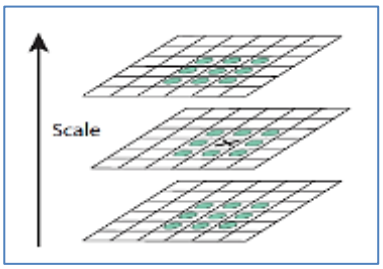

Figure 4. Feature localization.

- **Orientation assignment.** In this stage, orientation is assigned for each feature. This process results in rotational invariance for the descriptor. The image gradient directions of sample points around each key point are used to form an orientation histogram with 36bins. After testing different methods for assigning a local orientation, the best method is to use the scale of the key point to choose the Gaussian smoothed image, L, with the closest scale, so all computations are scale-invariant. Orientation, θ(x, y) in equation (4), and the gradient magnitude, m(x, y) in equation (5), at this scale are precomputed using pixel differences for each image sample, L(x, y), [13].

$$\theta(x,y) = \text{atan2}(L(x,y+1) - L(x,y-1), L(x+1,y) - L(x-1,y)) \quad (4)$$

$$m(x,y) = \sqrt{\left(L(x+1,y) - L(x-1,y)\right)^2 + \left(L(x,y+1) - L(x,y-1)\right)^2} \quad (5)$$

Where L(x, y) is the image sample, m(x, y) is the gradient magnitude, and θ(x, y) is the orientation.

- **Creating the feature descriptor.** This stage is the final step in SIFT. The aim of this stage is the creation of a unique fingerprint for each feature (key point) which has to be simple when we compare it against other features. So a 16x16 window is created around the feature [13]. This 16x16 window is broken into sixteen 4x4 windows figure 5.

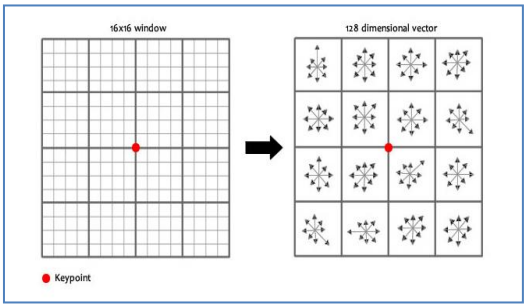

Figure 5. Feature descriptor.

The descriptor is a vector consisting of 128 elements that describe the area properties around the key point, which makes it invariant to remaining variations to match features and reject incorrect features. To increase the accuracy of the SIFT algorithm The Euclidean distance between features is used to reject the false positives by using the ratio between the closest neighbor and the second-closest neighbor Sometimes a correct match can have a larger distance than an incorrect match. In this case, we implement the nearest-neighbor distance ratio (NNR) which finds the nearest neighbor to the feature descriptor and the second nearest neighbor to the feature descriptor, and, divide the two as shown in equation (6).

$$NNDR=d1/d2 \tag{6}$$

Where d1 is the nearest neighbor distance and d2 is the second nearest neighbor distance.

3.3. The optimization method of the algorithm

We tested the optimized SIFT algorithm with different methods and software implementations, and finally, we used Fiji software, Fiji is an open-source software based on java; by using this software we can extract features for each image and identify the matched points in the two images and visualize the features also it gives us the ability to calculate the time of extracting and matching the features the result of each process can be saved for post-processing and analyzing data. The default parameters of SIFT work satisfactorily for many cases, but aerial images are considered bad textured because the dynamic range is quite low so stunning these parameters give us a better result [14]. SIFT has 17 parameters. Tuning all the parameters would be a very complex job, so authors usually select the most effective parameters for tuning [9]. We have deduced from our study and the suggestions made by [15] that the parameters sigma and N-Scales have a strong effect on the result [16]. So In this work, we tested different values for sigma, N-Scales and, NNR, as shown in table 1. The optimization, is made experimentally by scanning different values for the selected parameters which give the best possible match between the intended images. We also studied the effect of FDS on the selected images. The other parameters have been widely investigated extensively by other authors, so we used the default values recommended by Lowe. The efficiency of the proposed model was evaluated by analyzing the number of points matched (SM) and the correct match rate (CMR) as shown in equation (7). The algorithm is validated by matching a large number of aerial images with satellite images for the same region taking into consideration the processing time.

$$CMR = Ncorr/ Norig \tag{7}$$

Where N_{corr} is the number of correctly-matched points after eliminating false matches, and N_{orig} is the number of original points that are extracted in the first stage

Table 1. Optimized SIFT parameters in our study

Parameter	Default Values (Lowe)	Analysis range	Analysis Interval
sigma	1.6	0.1-2.6	0.1
N-Scales	3	3-9	1
NNR	0.8	0.8-0.92	0.01

3.3.1. Studying the effect of sigma parameter on SM, CMR, and time.

We tested range values of sigma parameter from 1 up to 2.6 on a large number of images, and we calculated the average of SM and CMR for all of these images as shown in figure 6 with taking into our consideration the time in figure 7.

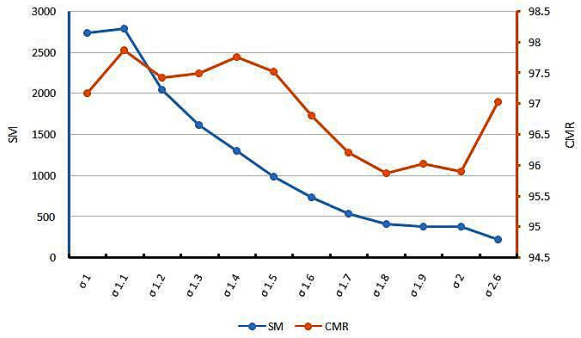

Figure 6. Calculating SM and CMR for different sigma values.

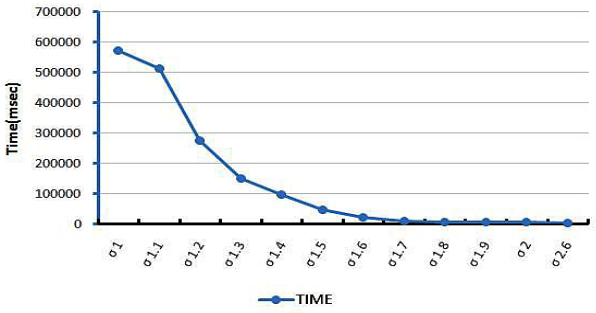

Figure 7. TIME for different sigma values.

From figure 6 and figure 7, we need the get sigma value at which we can get stable key points with reasonable time, so we can observe from figure 6 that increasing sigma value results in decreasing the number of points matched (SM) and this conclusion agree with the result of [17]. When we compare the sigma at value σ = 1.1 And 1.4 with the value of SM and CMR at these two points we find that the best value from this study is 1.4, Although the value of the SM at 1.1 is higher than the value at 1.4 are more, but this means that The stable key points at σ=1.4 are more than σ = 1.1 also when we take in our consideration the time in figure 7 we find that the sigma value at σ =1.4 is the best value from these two curves.

3.3.2. Studying the effect of N-Scales parameter on SM, CMR, and time.

From figure 8 and figure 9, we need to get the N-Scale value at which the highest value of SM and CMR is at a reasonable time. We tested the range values of the N-Scale parameter from 3 up to 9 on a large number of images. ImageJ recommends not using values of N-Scale ≥ 10 since they generate too many false matches that cannot be avoided using the RANSAC filter [14]. We calculated the average of SM and CMR for all of these images as shown in figure 8. We can observe from the curve in figure 8 the increasing N-Scale leads to an increase in the number of SM and consequently increase the processing time

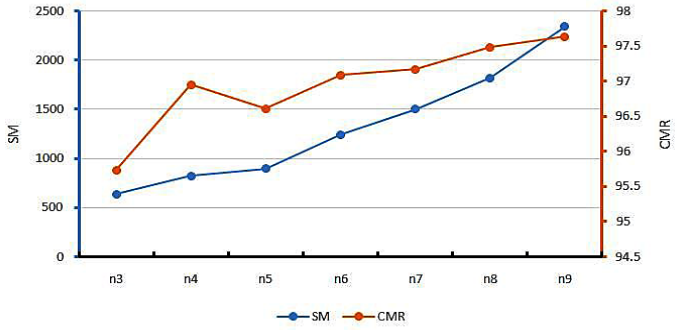

Figure 8. Calculating SM and CMR for different N-Scales.

From figure 9 we can observe the increasing time with the increasing number of SM

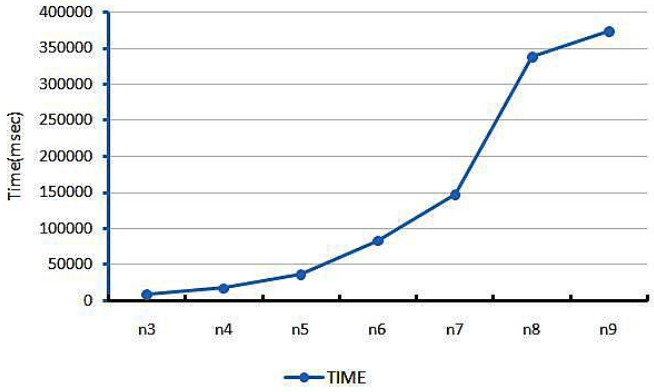

Figure 9. Calculating TIME for different N-Scales.

From the analysis of figure 8 and figure 9, we can observe that the highest value of SM and CMR is at N-Scale = 6 but the time is very high, so we selected N-Scale = 4 because the value of CMR at this scale is reasonable with time.

3.3.3. Studying the effect of N-scales parameter on SM, and CMR.

From figure 10 we study the effect of the NNR value; we studied the NNR range values on the imagery data set then we calculated the SM and CMR for each data set, after that, we calculated the average for these values.

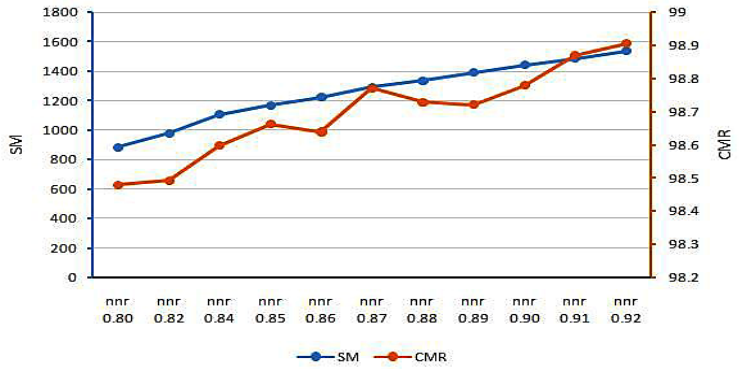

Figure 10. Calculating SM and CMR for different NNR values.

We can observe from figure 10 that the highest SM and CMR value is at NNR=0.92 and this agrees with the conclusion of [14].

3.4. Aerial platform

The aerial platform shown in figure 11 is a drone designed and manufactured for monitoring and reconnaissance applications.

Table 2. Technical specifications of the drone

Wingspan	170cm
takeoff weight	3KG
Endurance	90 min
Battery	10000mAh

The drone is a conventional configuration fixed-wing, electric power, pusher propeller-driven. This configuration gives the aerial vehicle superior flight performance.

Figure 11. Owl drone.

We fitted Pixhawk autopilot to the UAV, which is an open-source hardware autopilot for autonomous flight [12]. It is also equipped with a data link module (RFD900) to provide connectivity with the GCS

(ground control station) with operating frequency 900MHZ [15]. Mini OSD "On-Screen Display" is a small board that pulls the data from the autopilot and overlays it on the video link to be received on the video monitor on the ground [19]. The drone is equipped with a power module for monitoring volt and current consumption during the flight, an airspeed sensor, and a Lightbridge HD video link connected to a GoPro hero4 camera. This system gives us the capability to monitor and record video at 4K resolution [18]. In addition, a radio control transmitter (Spektrum dx8) is used to control the UAV manually (manual mode) or to change autopilot modes (AUTO –RTL-stabilize) [20].

3.5. Imagery sets

Two sets of images are used to test the algorithm and its optimization. The first set of images is captured with the UAV by using a GoPro hero4 camera as shown in figure 12. The camera specification is listed in table 3. The second set of images is taken from Google earth for the same area at different altitudes and different viewpoints as shown in figure 13. The specifications of this area are represented in table 5. The target of these types of Imagery sets is to evaluate the proposed parameters. These images were taken in October 2020 using the UAV. Picture in figure 12. The drone flies in auto mode at an altitude of 350:450m with a speed of about (9:15 m/s). In table 4 we can see the basic configuration of autopilot parameters.
The GoPro camera is configured to record video with a resolution of (1280 x 960).

Table 3. GoPro Hero 4 black

Waterproof housing	yes
Dimensions	41x59x30 mm
weight	152g
Video size/ max fps	4K/30fps – 2.7k/60 fps 1440p/80 fps 1080p/120fps 960p/120fps 720p/240 fps WVGA/240fps

Table 4. The basic configuration of autopilot parameters

Sea-level altitude	350-450 m
Pitch angel	-5 º to 17 º
Roll angel	45º

Table 5. Specifications of the satellite regions

Year	2018
Area	1000x600m
Eye alt	2464ft
Central coordinates	30º07`09.28"N 31º21`35.83"E
CITY	Cairo

Figure 12. Image captured by the GoPro hero4.

Figure 13. Image for the same area captured from Google earth.

4. Results and discussion

The optimization model is made experimentally by testing a range of SIFT parameters values in the process of image registration as was previously explained in table 1. The efficiency of the proposed model was evaluated by analyzing the number of points matched (SM) and the correct match rate (CMR). We choose random UAV images with the specifications stated in Table3. The UAV images are correlated with the satellite images. The specifications of the satellite regions specified in Table 5 and figure 12 show an aerial image selected randomly from the UAV images. This image for the same region of the satellite image is shown in figure 13. The UAV and satellite images show different orientations and scales. We have deduced from our study and the suggestions made by [Sima and Buckley. (2013)] that the two parameters sigma and N-Scales have a strong effect on the result. We also studied NNR and FDS effect on the data imagery set. The other parameters have been widely investigated extensively by other authors, so we used the default values recommended by Lowe. First, we studied the effects of these parameters on the selected images. Because the captured aerial images considered bad textured the results were not good as the proposed parameters, these results are shown in table 6. using RANSAC (random sample consensus) with the SIFT algorithm is to improve the accuracy of feature extraction by removing the mismatches also it helps in the avoidance of the high distortions produced by the camera lens of the UAV, so we used it with tolerance 10 pixels. It's clear from our study which is represented in table 6, figure 14, and figure 15 that the best result is from the proposed parameters which are the value of sigma is 1.4, N-scale 4, and The NNDR and FDS values are FDS = 8 × 8, NNDR = 0.92 as

recommended by ImageJ these values produce best results. Sigma and N-Scales values are not similar to the values proposed by Lowe and Castillo. Selecting of sigma value depends on the image quality. If the image is blurred we should use a lower sigma value, and this is agreed with the nature of the captured aerial images and the analysis in figure 6. The best value for sigma is 1.4. For N-Scale parameter increasing N-Scale parameter results in increasing the number of key points but it also increases the number of unstable key points which has a bad effect on the correct match rate, so we need to compromise between the number of key points and the number of stable key points with time so from figure 8 the best value for N-Scale is 4. Also, the FDS is 8x8 which achieves robustness against rotation and illumination change, and from figure 10we can deduce that the best value for NNR is 0.92.

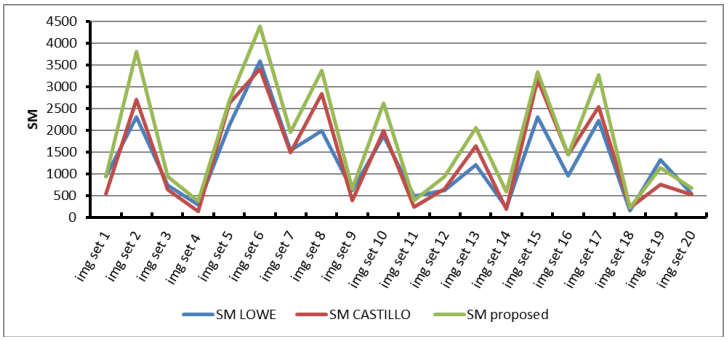

Figure 14. SM with different values of sigma, N-Scales, and FDS.

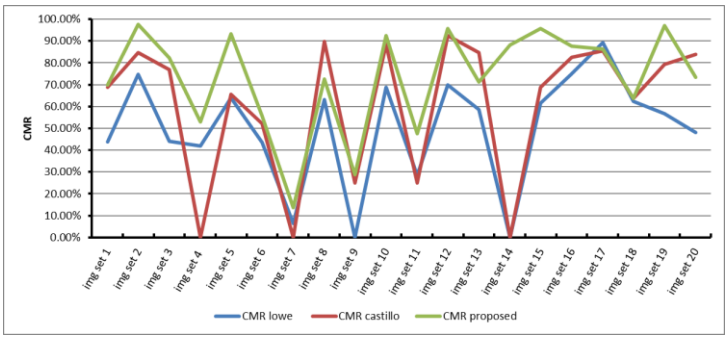

Figure 15. CMR with different values of sigma, N-Scales, and FDS.

We tested the proposed parameters, Lowe parameters [13], and Castillo [14] on several types of images. The results show that our optimized parameters (sigma, N-Scales, and FDS) give much better SM & CMR especially in aerial images as shown in figure 14 and figure 15.

Table 6. SM result for Lowe, Castillo and proposed parameters of different image sets

Method	parameters			Average no. of key points
Lowe	Sigma 1.6	N-Scale 3	FDS 4x8	1305
Castillo	Sigma 2.6	N-Scale 9	FDS 8x8	1410
Proposed parameters	Sigma 1.4	N-Scale 4	FDS 8x8	1794

By comparing the results in table 6, it becomes clear that the best result was achieved from the proposed parameters

4.1. Implementation of the proposed parameters practically on an image set

To confirm the process of registration with the proposed parameters practically we used two methods, the first one was to use the proposed parameters to extract the features for both UAV and Google satellite images then we analyzed the number of points matched (SM) and the correct match rate (CMR) for each of them then by using these features we aligned the UAV image with the satellite image for the same region as shown in figure 16. In the second method, we want to achieve redundancy in the process of registration, so we align multiple sequential frames taken from the video captured with the UAV with a single satellite image for the same region so we take a frame every 30 frames and use it in the process of registration as shown in figure 17.

a) Drone Image

b) Drone image (features)

C) Sat image

d) Sat Image (features)

e) Image matching and registration

Figure 16. Registration of Image captured with the drone (top) and image from Google satellite images

a) Sat Image

b) Sat Image (features)

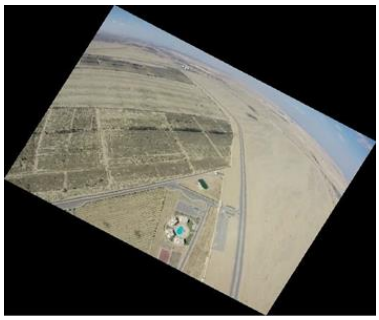

C) Frame no 1

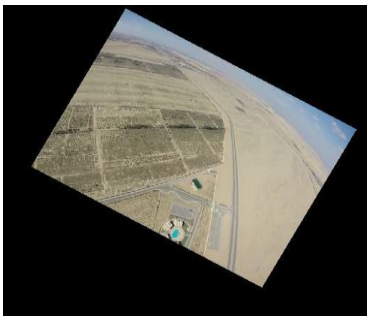

d) Frame no 2

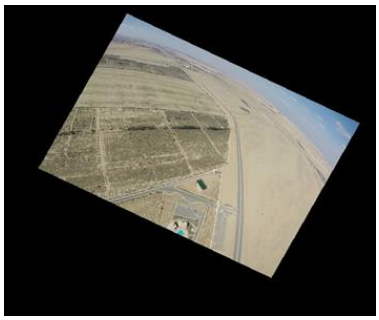

e) Frame no 3

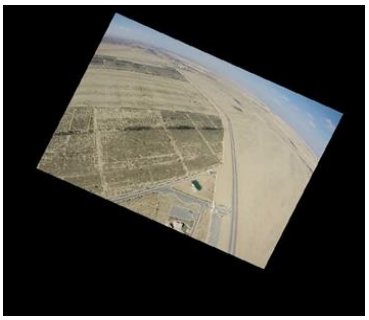

f) Frame no 4

Figure 17. The process of aligning frame every 30sec with satellite image for the same region (method 2).

5. Conclusions

In this paper, we tuned SIFT algorithm parameters to achieve the best results in the process of registration of matching UAV images with those from other sources such as satellite images from Google Earth. We focused in this study on Sigma, N-Scales, NNR, and FDS parameters because these are the most effective parameters. The other parameters value were kept fixed taking into consideration the proposed values by other authors under the same conditions. The efficiency of the proposed model was evaluated by analyzing the number of points matched (SM) and the correct match rate (CMR). It's clear from our study that the values of the optimized parameters are sigma is 1.4, N-Scale = 4, and The NNDR and FDS values are FDS = 8 × 8, NNDR = 0.92. These values produce the best results. Also, we used a RANSAC filter to avoid incorrect matches. With this approach, we could improve matching results between the UAV and the satellite images from Google Earth. These new parameters are validated by matching the aerial images taken by mini-UAV with satellite images for the same region.

Also, we tested the proposed parameters on multiple sequential frames taken from the video captured with the UAV with a satellite image for the same region. In future work, the optimization process will be automated.

References

[1] Zhong M, Zeng J and Xie X 2012 Panorama stitching based on SIFT algorithm and Levenberg-Marquardt optimization Physics Procedia **33** 811-818
[2] Hu M, Chen J and Shi C 2015 Three-dimensional mapping based on SIFT and RANSAC for a mobile robot. IEEE International Conference on Cyber Technology in Automation, Control, and Intelligent Systems 139-144
[3] Remondino F 2006 Detectors and descriptors for photogrammetric applications. International Archives of Photogrammetry, Remote Sensing and Spatial Information Sciences **36 (3)** 49-54
[4] James M and Robson S 2012 Straightforward reconstruction of 3D surfaces and topography with a camera: Accuracy and geoscience application. JOURNAL OF GEOPHYSICAL RESEARCH p 117
[5] Lingua A, Marenchino D and Nex F 2009 Performance analysis of the SIFT operator for automatic feature extraction and matching in photogrammetric applications. Sensors **9** 3745-3766
[6] Jinyan Tian, Xiaojuan Li, Fuzhou Duan, Junqian Wang and Yang Ou 2016 An efficient seam elimination method for UAV images based on wallis dodging and gaussian distance weight enhancement. Sensors **16** 662
[7] Yan K and Sukthankar R 2004 PCA-SIFT: A more distinctive representation for local image descriptors. Proceedings of the 2004 IEEE Computer Society Conference on Computer Vision and Pattern Recognition 506-513
[8] Ramanpreet Kaur, Puneet Mehta and Dishant Khosla 2017.A brief review on image stitching and panorama creation methods. International Journal of Control Theory and Applications **10** 327-336
[9] Yi Z, Zhiguo C and Yang X 2008 Multi-spectral remote image registration based on SIFT. Electronics Letters **44 (2)** 107–108
[10] Shuhan Chen, Shengwei Zhong, Bai Xue and Xiaorun Li 2020 Iterative scale-invariant feature transform for remote sensing image registration. IEEE Transactions on Geoscience and Remote Sensing **59** 3244-3265
[11] Wessel B, Huber M and Roth A 2007 Registration of near real-time SAR images by image-to-image matching. International Archives of Photogrammetry, Remote Sensing and Spatial Information Sciences **36** 179–184
[12] Nabeel Khan, Brendan McCane and Geoff Wyvill 2011 SIFT and SURF performance evaluation against various image deformations on benchmark dataset. International Conference on Digital Image Computing: Techniques and Applications 501-506
[13] Lowe DG 2004 Distinctive image features from scale-invariant keypoints. International Journal of Computer Vision **60** 91–110
[14] Castillo-Carrión S and Guerrero-Ginel J 2017 SIFT optimization and automation for matching images from multiple temporal sources. International Journal of Applied Earth Observation and Geoinformation **57** 113-122
[15] Sima A and Buckley S 2013 Optimizing SIFT for matching of short-wave infrared and visible wavelength images. Journal of Remote Sensing, **5** 2037-2056.
[16] May M, Turner M J and Morris T 2010 Object recognition from infrared image data for mobile platforms. MCM-ITP Conference **1** 29-40
[17] Park U, Pankanti S and Jain A 2008 Fingerprint verification using SIFT features. Biometric Technology for Human Identification, Proc.SPIE **6944** 69440K
[18] GoPro Hero 4 Black. 2020. Drone camera. Retrieved April 10, 2020, from https://gopro.com /en/us/

[19] Mini-OSD 2020 On-Screen Display. Retrieved April 10, 2020, from https://ardupilot.org/copter/docs/common-minim-osd-quick-installation-guide.html
[20] Pixhawk Flight Controller 2020 Pixhawk 1 Flight Controller. Retrieved April 22, 2020, from https://docs.px4.io/ v1.9.0/en/flight_ controller/pixhawk.html
[21] RFD900 2020 RFD900 long-range telemetry. Retrieved April 13, 2020, from https://docs.px4.io/v1.9.0 /en/telemetry/ rfd900_telemetry.html
[22] Spektrum DX8 2020 Radio control for RC planes. Retrieved March 5, 2020, from https://www.spektrumrc.com